

УДК 541(64+14):547.39

## SYNTHESIS AND CHARACTERIZATION OF NOVEL ALIPHATIC AMINE-CONTAINING DIMETHACRYLATE CROSS-LINKERS AND THEIR USE IN UV-CURABLE RESIN SYSTEMS<sup>1</sup>

© 2011 г. Guohe Hu <sup>a, b</sup>, Demei Yu <sup>a, b</sup>, Honglu Liang<sup>b</sup>, and Chao Min<sup>b</sup>

<sup>a</sup> State Key Laboratory of Electrical Insulation and Power Equipment, Xi'an Jiaotong University,  
Xi'an 710049, China

<sup>b</sup> School of Science, Xi'an Jiaotong University, Xi'an 710049, China  
e-mail: dmyu@mail.xjtu.edu.cn

Received July 4, 2010

Revised Manuscript Received November 2, 2010

**Abstract**—Two novel aliphatic amine-containing dimethacrylate monomers were synthesized from the ring-opening reaction of hexamethylene diamine and ethylenediamine with glycidyl methacrylate. The UV-curable and heat-curable formulations were prepared with amine-containing dimethacrylate and active diluents. The curing process was controlled by Fourier transform infrared analysis. The mechanical, physical, and thermal characterizations of the UV-cured films and the UV-heat-cured films were investigated. Thermo-gravimetric analysis of the cured films revealed that the thermo-oxidative stability of the UV-heat-cured films was higher than that of the UV-cured samples. An increase in the cross-linker content caused an increase both in tensile strength and in the elongation values of the UV-heat-cured films. It was also found that the water absorption capacities and gel content of the UV-heat-cured dimethacrylated films depended on the amount of the active diluents.

### INTRODUCTION

Utilization of UV-photoinitiated radical polymerization is continuously increasing because this technology has a lot of advantages, such as rapid cure, low energy consumption, high efficiency, and less environmental pollution [1–4]. It is widely used for coatings, printing inks, adhesives, and varnishes [5, 6]. UV-initiated photopolymerization systems generally consist of at least two major components: functional monomers, which are generally used to control the cross-linking density and viscosity, and a photoinitiator [7]. Most of the studies on UV-curable applications are focusing on free radical systems. These systems are based on acrylate monomers and their oligomers because they have high photopolymerization activities, which result to the production of cross-linked polymers with excellent mechanical and physical properties [8–14]. Monomers of this type, including dimethacrylates and trimethacrylates, are often referred to as base monomers and widely used in such UV photopolymerizations due to the monomer structure, which minimizes polymerization shrinkage by virtue of their relatively large molecular volume and also enhances the modulus of the cured networks [15]. The impact of multifunctional monomers in determining the final structures and physical properties of polymer networks has made them the subject of many investigations. Therefore, extensive studies have

shown that the photopolymerization of multifunctional monomers can result in unique reaction behaviors, such as unequal functional group reactivity and autoacceleration [16, 17].

However, the above-mentioned multifunctional monomer systems are inevitably affected by intermolecular forces, including hydrogen bonding. Jansen et al. [18, 19] investigated the rate of polymerization of different acrylates in terms of their hydrogen bonding capability in the systems, they found that the monomers which are capable of forming hydrogen bonds exhibit higher polymerization rates than their non-hydrogen-bonding analogs, which possessed ester and carbonate groups. They proposed that the high reactivities were due to preorganization via hydrogen bonding to bring the double bonds close to each other and enhance the rates of polymerization. Avci and Mathias [20] synthesized two hydroxyl-containing dimethacrylate monomers and investigated their polymerization behavior in the pendent moiety. They also found that the introduction of hydroxyl groups had an important effect on the bulk reactivities of these monomers. The formation of hydrogen bonding from the amine groups is feasible. However, amine-containing dimethacrylate monomers had not been discussed well in their systems [21, 22]. Recently, Bergiers et al. [23] synthesized amino (meth)acrylates obtained from the Michael addition reaction of acrylates and amine and used it for making flexible varnishes, coatings, adhesives and inks. In this work, we synthesized two

<sup>1</sup> Статья печатается в представленном авторами виде.

**Table 1.** Viscosity of the cross-linkers

Temperature, °C	Viscosity, mPa s	
	EDA-GMA	HDA-GMA
25	33500	32000
30	12000	13000
40	8200	8400
50	3600	3800
60	1700	1500
70	1600	1320
80	1970	1900
90	2300	2240

**Table 2.** TGA results of the cured film

Cross-linker	Recipe*	5% loss temperature, °C	Decomposition temperature, °C
HDA-GMA	20/20/58/2**	235	330
	20/15/63/2	298	344
	20/20/58/2	298	345
	20/25/53/2	302	348
	20/30/48/2	305	349
	20/20/58/2**	235	332
EDA-GMA	20/15/63/2	302	340
	20/20/58/2	300	345
	20/25/53/2	305	349
	20/30/48/2	308	350

\* The numbers used in the tables represent the weight percentage contents of the cross-linkers, GMA, BA, and photoinitiator, respectively.

\*\* UV-cured films.

amine-containing dimethacrylate monomers from the ring-opening reaction of glycidyl methacrylate (GMA) to aliphatic diamine. We also investigated the essential reaction parameters in relation to the properties that may be useful in the applications of the dimethacrylate polymer films.

## EXPERIMENTAL

### Materials

Glycidyl methacrylate (GMA) (ShangHai JiYuan Chem. Co., China) was distilled under reduced pressure. Hexamethylene diamine (HDA), ethylenediamine (EDA), butyl acrylate (BA), and methylene dichloride were of analytical grade and used without any purification. Reagent grade Irgacure 184 (1-hydroxycyclohexyl phenyl ketone) was supplied from Ciba Specialty Chemicals (Switzerland).

### Synthesis of the Cross-linker Agent

The procedure of the synthesis adducts is followed. To a solution of GMA in dichloromethane, hexamethylene diamine (or ethylenediamine) and zinc perchlorate-alumina was added. The mole ratio of GMA to diamine was 2 : 1. The reaction mixture was stirred at room temperature for 5–8 hours using the  $Zn(ClO_4)_2-Al_2O_3$  catalyst system, and the resulting adduct was distilled under reduced pressure. The catalyst system has been reported in [24]. The reaction was controlled by the change of epoxide number and FTIR analysis. EDA-GMA and HDA-GMA were prepared from ethylenediamine and hexamethylene diamine, respectively (Scheme 1). Each synthetic monomer was isolated by silica gel column chromatography and then concentrated in vacuo. The viscosity of these adducts under different temperatures was also studied using an NDJ-4 rotational viscometer (Shanghai Balance Instrumental Manufacture) (Table 1).

### Curing Procedure

The formulations of UV-curable films were prepared as follows. Generally, the EDA-GMA or HDA-GMA adduct was added to a solution of GMA and BA. Then, 2 wt% photoinitiator (Irgacure 184) was added into the mixture. The details of the formulations are given in Tables 2 and 3. The mixture was stirred at 60–70°C for 4 h. Then, polymeric films approximately 300 μm thick were prepared by pouring the mixture into a mold that was preheated to over 50°C. Finally, the mixture was cured by exposure to a high-pressure UV lamp (LT-102, 1 kW) for about 70 s at room temperature. The exposure time of 70 s was initially determined in a separate experiment on optimization of the mechanical properties. More than one method can be used to prepare the formulations. Most of the formulations were postcured at 120°C for 2 h after UV cured (unless otherwise noted).

### Characterizations

The infrared (IR) spectra of the cross-linkers were measured in KBr pellets using a NICOLET Fourier transform infrared (FTIR) spectrometer. The films of samples were taken by an attenuated total reflectance (ATR) accessory.

Differential scanning calorimetric (DSC) thermograms of the resulting HDA-GMA and EDA-GMA adducts were obtained using a Netzsh DSC 200PC equipped with a refrigeration cooling system. The furnace was purged with dry nitrogen at a flow rate of 20 ml/min. The samples (5–10 mg) were heated continuously from –155 to 150°C at a heating rate of 10 K/min. Thermogravimetric analysis (TGA) was performed using a Netzsh TG 209 thermogravimetric analyzer at a heating rate of 20°C/min in air.

**Table 3.** Properties of EDA-GMA-based polymeric films

Recipe*	Gel content, %	Water absorption, %	Breaking strength, MPa	Elongation at break, %
20/15/63/2	87.4	2.96	4.45	15.54
20/20/58/2	89.2	2.38	5.47	30.74
20/20/58/2**	65.9	9.89	2.77	24.77
20/25/53/2	91.0	2.14	5.34	14.02
20/30/48/2	93.1	2.01	8.98	18.91
20/30/48/2**	78.0	8.75	2.63	28.35
20/40/38/2	91.7	1.81	10.02	2.81
20/45/33/2	90.6	1.74	11.16	0.98
25/15/58/2	90.1	2.33	5.13	15.03
25/20/53/2	91.6	1.62	9.01	18.65
25/25/48/2	93.6	1.44	7.24	5.01
25/30/43/2	94.7	1.41	9.76	0.89

\* The numbers used in the tables represent the weight percentage contents of the cross-linkers, GMA, BA, and photoinitiator, respectively.

\*\* UV-cured films.

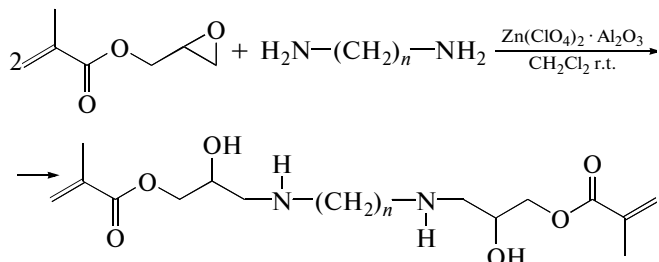
The gel content of the samples was determined using a Soxhlet extractor for 12 h with an acetone solution. The insoluble gel fraction was dried at 70°C in a vacuum for 24 h and weighed to calculate the gel content.

The water absorption capacities of the samples were determined by immersing the samples in deionized water at room temperature for 24 h. The weight difference between the dry films and the films soaked in water was calculated.

The mechanical properties of the UV-curable and heat-curable films were determined by standard tensile stress-strain tests to measure the ultimate tensile strength and elongation at breaking. A tensile testing machine (ShenZhen SANS, China) was operated according to the China standard GB/T 13022–1991 using a cross-head rate of 20 mm/min at room temperature. All stress-strain measurements were done in triplicate.

## RESULTS AND DISCUSSION

### Characterizations of the Cross-linkers



**Scheme 1.** Synthesis of EDA-GMA ( $n = 2$ ) and HDA-GMA ( $n = 6$ ).

The synthetic route for the diamine-GMA adducts is presented in Scheme 1. The FTIR spectra of GMA and the adducts are presented in Fig. 1. The IR spectra showed bands at 3200–3600 cm<sup>-1</sup>, confirming the formation of hydroxyl groups. There were also bands at 1613 and 1609 cm<sup>-1</sup>, confirming the formation of vinyl groups. Combined with the disappearance of the bands at 850 and 905 cm<sup>-1</sup>, which are typical for epoxide, these results confirmed the success of the addition reaction. As we know, Michael addition reaction between aliphatic amines and acrylic esters is likely to occur. However, the experiments showed a higher yield above 80% may be due to the presence of the regioselective catalyst  $Zn(ClO_4)_2 \cdot Al_2O_3$  and the experi-

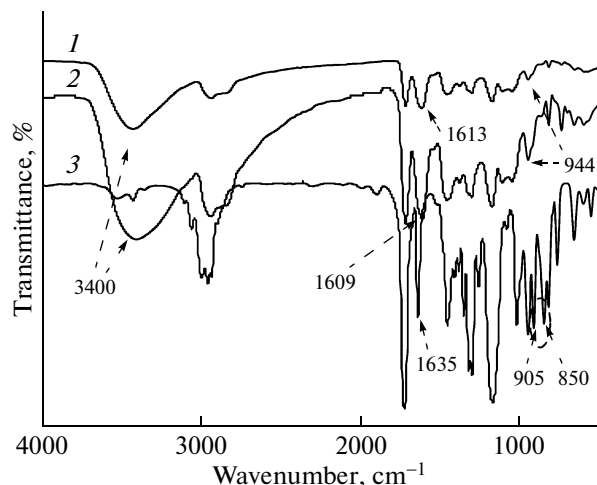


**Fig. 1.** FTIR spectra for these adducts and glycidyl methacrylate: EDA-GMA (1), HDA-GMA (2), GMA (3).

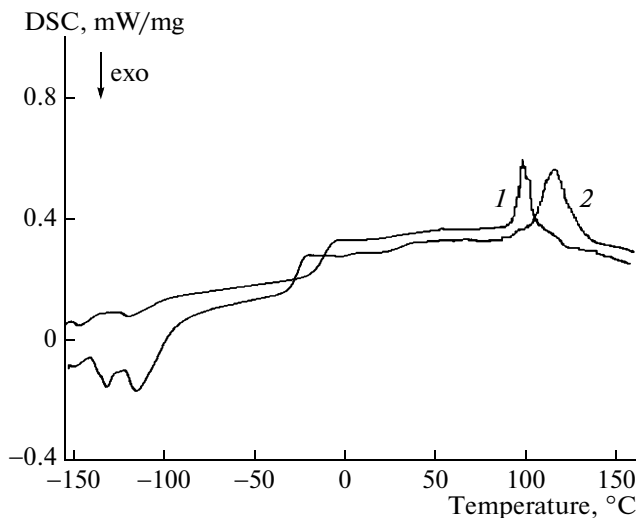


**Fig. 2.** DSC analysis for EDA-GMA (1) and HDA-GMA (2) adducts.

mental system. The IR peak at  $1635\text{ cm}^{-1}$  red-shifted to  $1609$  and  $1613\text{ cm}^{-1}$ , indicating the characteristic peaks of the vinyl group.

Figure 2 presents DSC thermograms of EDA-GMA and HDA-GMA recorded at a heating rate of  $10\text{ K/min}$  after a previous cooling of about  $15\text{ K/min}$ . The thermograms showed an endothermic peak characteristic of a glass transition state appeared at a temperature  $-20^\circ\text{C}$ . The  $T_g$  of EDA-GMA and HDA-GMA were  $-12.5$  and  $-26.8^\circ\text{C}$ , determined as the temperature of the midpoint of the heat capacity increment in transition, while the increment in the heat capacity of the glass transition were  $0.613$  and  $0.624\text{ J/g}$ , respectively. The glass transitions were quite broad, covering roughly the same value ( $\Delta T_g = 6.5^\circ\text{C}$ ). At a lowest temperature, there are two exothermal peaks below glass transition temperature of both EDA-GMA and HDA-GMA, and were suspected of the crystallizations peaks. Maybe they are due to the intermolecular and intramolecular hydrogen bonding forces, which resulted to a local molecular at a lowest temperature. At a higher temperature, broad endothermic peaks for both EDA-GMA and HDA-GMA were observed due to melting. The areas had a broad melting peak with endothermic areas measured at around  $4.19$  and  $4.26\text{ J/g}$  for EDA-GMA ( $100$  to  $115^\circ\text{C}$ ) and HDA-GMA ( $110$  to  $130^\circ\text{C}$ ), respectively. At a temperature higher than the melting temperature, both adducts approached exothermal polymerization.

From Fig. 3 we can see that the thermal degradation behavior of EDA-GMA and HDA-GMA. In the derivative of the TGA curves, two main characteristic weight loss peaks were observed. The first stage of degradation was located at  $95\text{--}100^\circ\text{C}$ , which probably corresponded to the volatilization of the degradation products, such as the entrapped moisture or diluents.

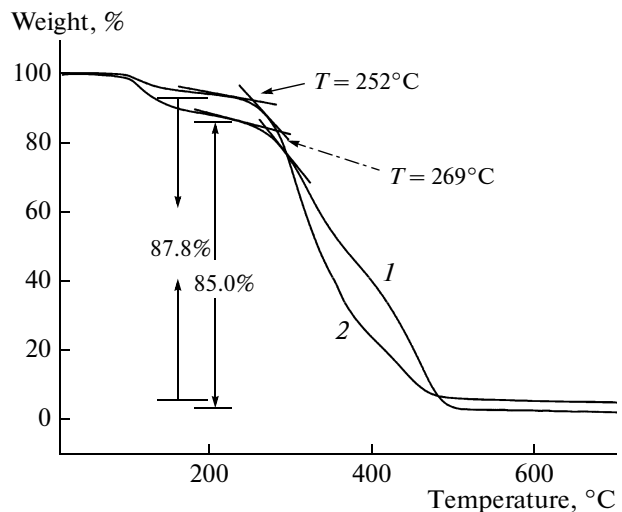


**Fig. 3.** TGA thermograms of EDA-GMA (1) and HDA-GMA (2) adducts.

Interestingly, there were gentle slopes for weight loss in the second stage of degradation for both adducts. These occurred before  $252$  and  $269^\circ\text{C}$  for EDA-GMA and HDA-GMA, respectively. As mentioned in the DSC analyses, these gentle slopes of weight loss were probably due to the polymerization since they occurred at a temperature higher than the melting temperature.

The viscosities of the two adducts are listed in Table 1. From these data, one can see that the viscosity was rather high at low temperatures. However, the viscosity initially decreased and then increased as the temperature was raised. In the comparative DSC analysis, even though the compound was close to a melting state at  $60\text{--}70^\circ\text{C}$ , the compounds in the air already began to polymerize at this time, resulting in an increased viscosity.

#### Properties of the Cured Film

Figure 4 shows the original spectra of the UV-cured and UV-heat-cured film with a weight ratio of  $20/30/48/2$  and HDA-GMA as the cross-linker. According to the Beer-Lambert law, the intensity of a band is in direct proportion to the concentration of the sample. The intensity at  $756\text{ cm}^{-1}$ , associated with the deformation mode of hexylidene  $(\text{CH}_2)_6$  [25, 26] in HDA-GMA, was used as a reference because the content of HDA-GMA was held constant in the experiments. Hence, the relative intensities of the  $845$  and  $907\text{ cm}^{-1}$  bands in the UV-heat-cured films were decreased with respect to the film prepared only with UV curing. Meanwhile, the intensity of the characteristic peak of the hydroxyl group at  $3400\text{ cm}^{-1}$  increased in the UV-heat-cured films compared with the UV-cured films. These results imply that a combination of

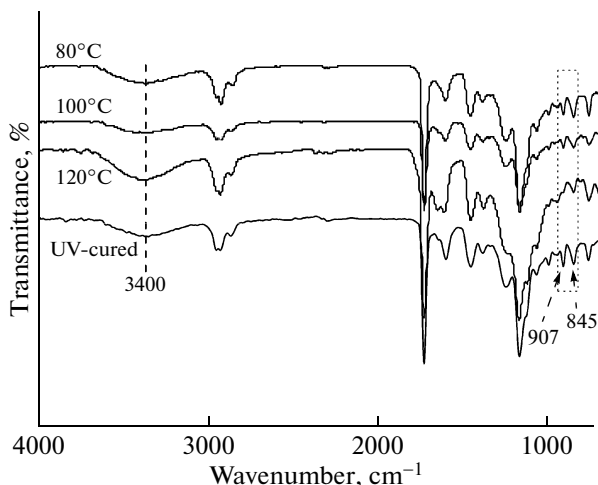


**Fig. 4.** FTIR spectra of the copolymers prepared with the formulation 20/30/48/2 and HDA-GMA as a cross-linker after photoinitiation by UV light at different temperatures.

UV and heat curing gives better polymerization than only UV-initiated polymerization.

As mentioned, the intensity of the 756 cm<sup>-1</sup> band was nearly unchanged during curing because the content of HDA-GMA was constant, whereas the intensities of the 850 and 907 cm<sup>-1</sup> bands associated with the deformation mode of the epoxy group decreased as the curing process progressed. The trend of the intensity of the 850 cm<sup>-1</sup> band is shown in Fig. 5.  $A_{850}$  and  $A_{756}$  are

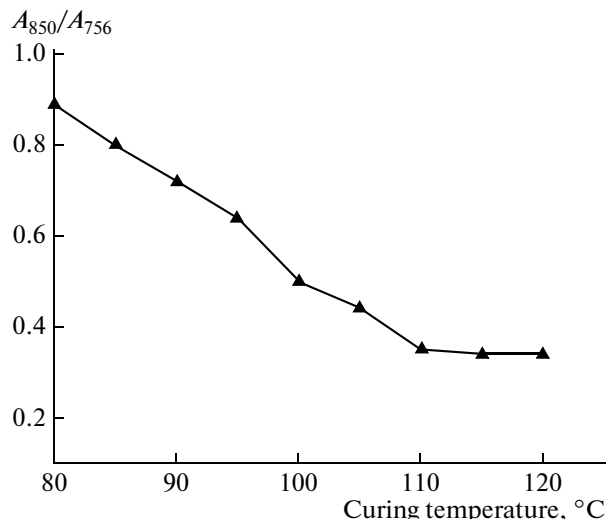


**Fig. 5.** Dependence of normalized integral intensity of the 850 cm<sup>-1</sup> band on curing temperature.

the normalized areas of the 850 and 756 cm<sup>-1</sup> bands, respectively. The relative intensity of the value stabilized as the temperature reached 120°C.

The thermal degradation behaviors of HDA-GMA- and EDA-GMA-based polymeric films were assessed by TGA in an air atmosphere. Figure 6 shows a TGA thermogram of a film containing 20% HDA-GMA cross-linking agents. It can be seen that all UV-heat-cured samples showed an approximately 5%

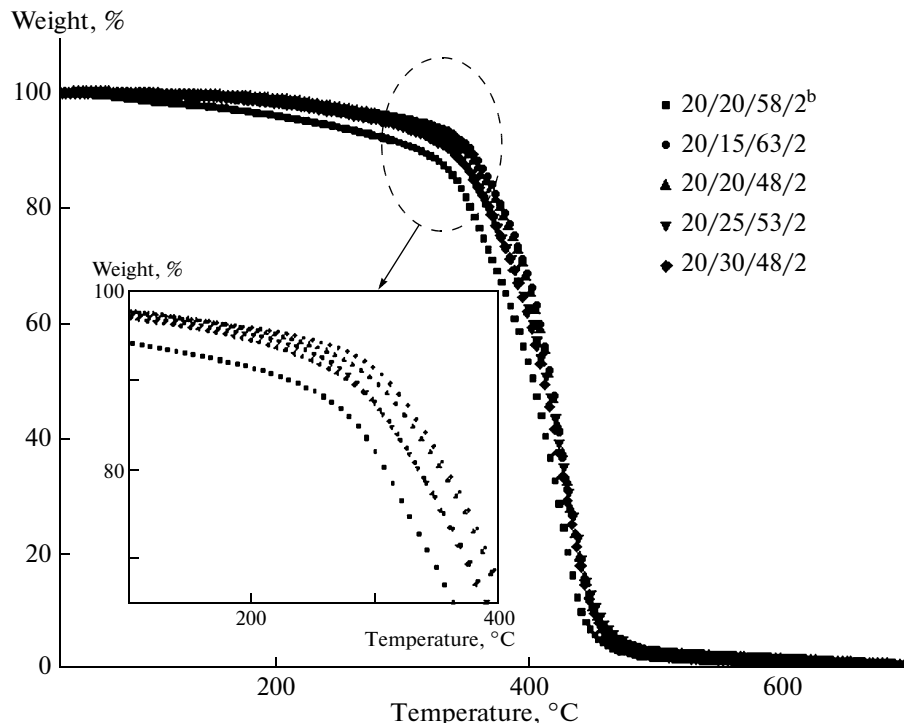


**Fig. 6.** TGA thermograms of film containing 20% HDA-GMA cross-linking agents.

**Table 4.** Properties of HDA-GMA-based polymeric films

Recipe*	Gel content, %	Water absorption, %	Breaking strength, MPa	Elongation at break, %
20/15/63/2	90.57	2.71	4.21	11.67
20/20/58/2	91.6	2.31	5.70	20.74
20/20/58/2**	68.8	9.67	2.23	24.97
20/25/53/2	93.7	2.02	5.45	13.86
20/30/48/2	96.3	1.96	9.82	20.07
20/30/48/2**	73.6	8.89	2.85	21.27
20/40/38/2	92.13	1.87	9.98	3.08
20/45/33/2	91.02	1.64	11.03	1.01
25/15/58/2	89.8	1.09	5.40	16.21
25/20/53/2	82.1	1.44	9.34	18.88
25/25/48/2	94.3	1.53	6.67	4.58
25/30/43/2	98.8	1.02	10.57	0.93

\* The numbers used in the tables represent the weight percentage contents of the cross-linkers, GMA, BA, and photoinitiator, respectively.

\*\* UV-cured films.

weight loss at around 300°C and decomposed rapidly at around 350°C, while the UV-cured samples exhibited a 5% weight loss at around 235°C and decomposed rapidly at 330°C. Apparently, the thermo-oxidative stability of the UV-heat-cured film was higher than that of the UV-cured sample. According to a previous analysis, the amino groups of the cross-linking agent were considered to be involved in the epoxy ring-opening reaction in the heat curing stage, resulting to the formation of the network structure and enhancement of the thermo-oxidative stability. When EDA-GMA was used as a cross-linking agent, it had similar results (Table 2). The thermo-oxidative stability of the UV-heat-cured film was also better than that of the UV-cured sample.

The compositions of the UV-cured dimethacrylated films were changed by varying the content of the cross-linker and two reactive diluent co-monomers while keeping the amount of photoinitiators constant. The amount of the synthetic cross-linker was found to have a considerable effect on the mechanical properties of the UV-cured polymeric films. The stress-strain values for the two cross-linkers are given in Tables 3 and 4. The gel contents of the UV-cured films were found to be up to 78% lower than that of the UV-heat-cured films. The water absorptions of the UV-cured films were higher than that of the UV-heat-cured formulations. These results imply that the cross-linking density of the UV-cured films was lower than that of the UV-heat-cured films. An increase in the cross-linker content caused an increase in the ultimate tensile strength in all the films. Increasing the cross-linking agent increased the hard segment content and cross-linking density. A comparison of the mechanical properties of the samples showed that the ultimate break strength increased when the amount of cross-linker

was kept constant at 20 wt%. The change in the tensile strength values might have resulted from more ring-opening reaction between EDA-GMA or HDA-GMA and the epoxy groups of GMA when the content of the latter was increased. The GMA molecules in the network acted as co-monomers and resulted to greater cross-linking density and tensile strength prior to breaking. Consequently, the cured films became more brittle. A similar behavior was also observed for the water absorption. An increase in the cross-linking density meant less water was trapped in the polymer network. The gel content of the cured films initially increased and then decreased with the increase in GMA because unreacted GMA molecules acted as plasticizers in the network when it was increased to excess amounts.

#### ACKNOWLEDGMENTS

This work was financially supported by Grant No. 2009CB724202 from China's National "973" Program.

#### REFERENCES

1. T. Yilmaz, Ö. Özarslan, E. Yıldız, A. Kuyulu, E. Ekinci, and A. Güngör, *J. Appl. Polym. Sci.* **69**, 1837 (1998).
2. K. Maruyama, H. Kudo, T. Ikehara, N. Ito, and T. Nishikubo, *J. Polym. Sci. Part A* **43**, 4642 (2005).
3. M. Sangermano, G. Malucelli, E. Amerio, A. Priola, E. Billi, and G. Rizza, *Prog. Org. Coat.* **54**, 134 (2005).
4. A.S. Sawhney, C.P. Pathak, and J.A. Hubbell, *Macromolecules* **26**, 581 (1993).
5. N. Kayaman-Apohan, A. Amanoel, N. Arsu, and A. Güngör, *Prog. Org. Coat.* **49**, 23 (2004).
6. J.X. Feng, L.J. Zhu, C.M. Lu, S.L. Teng, M.W. Young, and C.G. Gogos, *Polym. Eng. Sci.* **49**, 1107 (2009).

7. T.Y. Inan, Ö. Özarslan, A. Kuyulu, E. Ekinci, and A. Güngör, *J. Appl. Polym. Sci.* **73**, 2575 (1999).
8. R. Schwalm, L. Häußling, W. Reich, E. Beck, P. Enenkel, and K. Menzel, *Prog. Org. Coat.* **32**, 191 (1997).
9. G. Bayramoglu, M.V. Kahraman, N.K. Apohan, and A. Gungor, *Polym. Adv. Tech.* **18**, 173 (2007).
10. D.K. Chattopadhyay, S.S. Panda, and K.V.S.N. Raju, *Prog. Org. Coat.* **54**, 10 (2005).
11. S.W. Zhu and W.F. Shi, *Polym. Degrad. Stab.* **82**, 435 (2003).
12. A.A. Stolov, T. Xie, J. Penelle, S.L. Hsu, and H.D. Stidham, *Polym. Eng. Sci.* **41**, 314 (2001).
13. K.S. Anseth, L.M. Kline, T.A. Walker, K.J. Anderson, and C.N. Bowman, *Macromolecules* **28**, 2491 (1995).
14. A.R. Kannurpatti, J.W. Anseth, and C.N. Bowman, *Polymer* **39**, 2507 (1998).
15. E. Andrzejewska, *Polymer* **37**, 1039 (1996).
16. J.W. Stansbury and S.H. Dickens, *Polymer* **42**, 6363 (2001).
17. G.J. Sun and K.H. Chae, *Polymer* **41**, 6205 (2000).
18. J.F.G.A. Jansen, A.A. Dias, M. Dorsch, and B. Cousens, *Polym. Prepr.* **42**, 769 (2001).
19. J.F.G.A. Jansen, A.A. Dias, M. Dorsch, and B. Cousens, *Macromolecules* **36**, 3861 (2003).
20. D. Avci and L.J. Mathias, *Polymer* **45**, 1763 (2004).
21. B. Gawdzik, T. Matynia, and O. Kovtun, *J. Appl. Polym. Sci.* **95**, 524 (2005).
22. A. Drelinkiewicz, A. Knapik, W. Stanuch, J. Sobczak, A. Bukowska, and W. Bukowski, *React. Funct. Polym.* **68**, 1652 (2008).
23. Bergiers, Francis, Randoux, and Thierry, PCT Patent EP2007/056238 (2008).
24. M. Maheswara, K.S.V.K. Rao, and J.Y. Do, *Tetrahedron Lett.* **49**, 1795 (2008).
25. Y.L. Lu, L. Liu, D.Y. Shen, C. Yang, and L.Q. Zhang, *Polym. Int.* **53**, 802 (2004).
26. C.S. Zhu, *Polymer Structure Analysis* (Science Press, Beijing, 2004).